

# Wireless Transmission of Images With The Assistance of Multi-level Semantic Information

Zhenguo zhang, Qianqian Yang, Shibo He, Mingyang Sun, Jiming Chen  
Zhejiang University, Zhejiang, China

{zhangzhenguo, qianqianyang20, s18he, mingyangsun, cjm}@zju.edu.cn

**Abstract**—Semantic-oriented communication has been considered as a promising to boost the bandwidth efficiency by only transmitting the semantics of the data. In this paper, we propose a multi-level semantic aware communication system for wireless image transmission, named MLSC-image, which is based on the deep learning techniques and trained in an end to end manner. In particular, the proposed model includes a multi-level semantic feature extractor, that extracts both the high-level semantic information, such as the text semantics and the segmentation semantics, and the low-level semantic information, such as local spatial details of the images. We employ a pre-trained image caption to capture the text semantics and a pre-trained image segmentation model to obtain the segmentation semantics. These high-level and low-level semantic features are then combined and encoded by a joint semantic and channel encoder into symbols to transmit over the physical channel. The numerical results validate the effectiveness and efficiency of the proposed semantic communication system, especially under the limited bandwidth condition, which indicates the advantages of the high-level semantics in the compression of images.

## I. INTRODUCTION

Shannon’s separation theorem is the cornerstone of the traditional communication system [1], serving as a design criterion to establish modern wireless communication framework from the first-generation (1G) to the fifth-generation (5G). With the rapid development of wireless communication, the communication system channel capacity is close to the Shannon limit. Researchers have been exploring ways to go beyond Shannon capacity to meet the rapid-growing demands of wireless data transmission, and the semantic oriented communication system has been well recognized as a promising approach for the next generation wireless communication [2]–[4].

In contrast to traditional communication, semantic communication focuses on the transmission of the meaning of the information, instead of the exact transmission of symbols. The existing semantic communication systems jointly design the transmitter and receiver to achieve better transmission efficiency and robustness to the changing of channel conditions [5], [6]. Deep learning (DL) based semantic communication systems have revealed tremendous potential in the efficient transmission of different types of information, i.e., text [7]–[9], speech [10], [11], and image [12]–[18].

This work is partly supported by National Key R&D Program of China under the project 2020YFB1708700, partly by the SUTD-ZJU IDEA Grant (SUTD-ZJU (VP) 202102), and partly by the Fundamental Research Funds for the Central Universities under Grant 2021FZZX001-20.

For the semantic compression and transmission of the images, DL has been applied to optimal conventional image compression [13], which proposes a two-step method by combining the state-of-the-art signal processing-based recovery method with a deep residual learning model to recover the original image. Eirina *et al.* [12] propose a DL based wireless image transmission system to achieve joint source-channel coding in an end to end manner, where peak signal-to-noise ratio (PSNR) and structure-similarity-index-measure (SSIM) are devoted to measuring the quality of the reconstructed images. Based on JSCC, another image reconstruction scheme with channel feedback, named DeepJSCC-f, has been implemented [14] to enhance image reconstruction accuracy with feedback from the receiver. Yanget *al.* [15] present a JSCC scheme with an OFDM datapath for wireless image transmission over multipath fading channels. Moreover, the proposed model achieves remarkable performance by integrating expert knowledge. The progressive research on internet Internet-of-Things (IoT) devices for image transmission has developed in [16], which proposed a joint transmission-recognition scheme leveraging two DNNs, which outperforms the conventional scheme at the IoT devices. Mikolaj *et al.* [17] present a joint feature compression and transmission system to deal with the limited computational resources at the edge server, named DeepJSCC, which not only improves end-to-end reliability but also reduces computation complexity. Mikolaj *et al.* [18] proposes an autoencoder-based system for device-edge communication with rigorous constraints, which achieves better performance in classification accuracy with limited computation capacity.

In this work, we propose a novel DL-based semantic communication system for image transmission over noisy wireless channels. In particular, we introduces a multi-level semantic feature extractor, that exploits both the high-level semantic information including the text semantic information and segmentation semantic information, which contains abstractedness and generality indication of an image [19], and the low-level semantic information, such as local details of the image. The numerical results shows that the proposed method remarkably outperform the existing method in high to medium compression ratio, which validates the semantic significance of the high-level semantic information.

The rest of the paper is organized as follows. In Section II, we introduce the system model. The details of the architecture

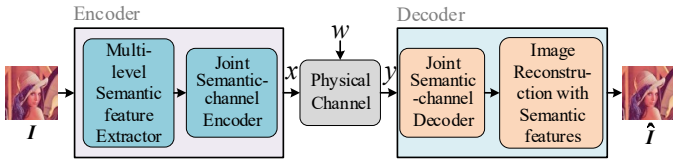


Fig. 1. The proposed semantic-oriented communication of image.

are shown in III. Section IV presents the numerical results, and Section V concludes the paper.

## II. SYSTEM MODEL

### A. System Description

We consider a semantic communication system, as shown in Fig. 1, where the transmitter sends an image to the receiver over a physical channel. The system consists of two parts: (i) the encoder at the transmitter, which extracts semantic features from the input image and encodes them to symbols to transmit over the channel; and (ii) the decoder at the receiver, which decodes the semantic features from the received signals to reconstruct the input image from them. We will describe the encoder and decoder in details in the sequel.

### B. Encoder

The encoder consists of two components: the multi-level semantic feature extractor and the joint semantic-channel encoder. The input image  $I$  to the encoder is preprocessed by a normalization layer such that each element is in the range of  $[0,1]$ . Then the multi-level semantic feature extractor, which contains multiple NN-based modules, extracts different semantic features of the input image. The joint semantic-channel encoder encodes these semantic features into symbols to transmit over the physical channel to the receiver. Denote the NN parameters of the multi-level semantic feature extractor and the joint semantic-channel encoder as  $\alpha$ , and  $\beta$ , respectively. Then the signal symbol vector to be transmitted  $\mathbf{x}$  is given:

$$\mathbf{x} = \mathbf{T}_\beta^c(\mathbf{T}_\alpha^i(I)), \quad (1)$$

where  $\mathbf{T}_\alpha^i(\cdot)$  denotes the operation by the multi-level features extracting network with parameters  $\alpha$ , and  $\mathbf{T}_\beta^c(\cdot)$  is the joint semantic-channel encoder function with parameter  $\beta$ .

We consider a widely used physical channel: the AWGN channel. We have the received signal at the decoder given as:

$$\mathbf{y} = \mathbf{h}\mathbf{x} + \mathbf{w}, \quad (2)$$

where  $\mathbf{h}$  represents the channel coefficients,  $\mathbf{w}$  is a vector of independent identically distributed (i.i.d.) channel noise following a circularly symmetric Gaussian distribution, i.e.,  $\mathbf{w} \sim \mathcal{CN}(0, \sigma^2 \mathbf{I})$ ,  $\sigma^2$  is the average noise power of the channel, and  $\mathbf{I}$  is the identity matrix.

### C. Decoder

The decoder consists of two parts, the joint semantic-channel decoder and the image reconstruction module. The joint semantic-channel decoder mitigates physical noise in the received signal collected over the AWGN channel and recovers the multi-level semantic features. The image reconstruction module fuses the different levels of semantic information and reconstructs the target image. Finally, the denormalization layer rescales each element to image pixel values (0-255).

The parameter sets of the joint semantic-channel decoder and the image reconstruction module are denoted by  $\zeta$  and  $\eta$ , respectively. The reconstructed image at the receiver from the received signal is given by:

$$\hat{I} = \mathbf{R}_\eta^r(\mathbf{R}_\zeta^c(\mathbf{y})), \quad (3)$$

where  $\mathbf{R}_\zeta^c(\cdot)$  and  $\mathbf{R}_\eta^r(\cdot)$  denote the operation of the joint semantic-channel decoder and the image reconstruction module, respectively.

The goal of the considered semantic communication system is to minimize the average distortion between input image  $I$  and reconstructed image  $\hat{I}$ . The mean-squared-error (MSE) is used as the loss function to evaluate the distortion between  $I$  and  $\hat{I}$ , denoted as:

$$\mathcal{L} = \frac{1}{N} \sum_{k=1}^N d(\mathbf{I}_k, \hat{\mathbf{I}}_k), \quad (4)$$

where  $d(\mathbf{I}, \hat{\mathbf{I}}) = \frac{1}{n} \|\mathbf{I} - \hat{\mathbf{I}}\|^2$  is the MSE distribution, and  $N$  is the number of samples.

## III. PROPOSED METHOD

We present the proposed DL-based semantic communication system for wireless image transmission, as shown in Fig. 2, referred to as MLSC-image. Specifically, the multi-level semantic feature extractor is used for extracting different levels of semantic features. The joint semantic-channel encoder and decoder successfully recover these features at the receiver. Then the image reconstruction module is adopted to fuse the multi-level semantic information so that to reconstruct the target image.

### A. Multi-level Semantic Feature Extractor

The input of the proposed MLSC-image scheme, denoted as  $\mathbf{I} \in \mathfrak{R}^{b \times h \times w \times 3}$ , is a batch of image samples, where  $b$ ,  $h$ , and  $w$  are the batch size, the image height, and width, and the last dimension correspond to the RGB channels. The image is first preprocessed by a normalization layer to scale the value of the pixel to  $[0,1]$ . The normalized image batch is then input to the multi-level semantic feature extractor, which consists of three-level feature extraction modules: the semantic feature module, the segmentation feature module, and the low-level feature module. The semantic feature module contains a pre-trained image caption model to acquire text-form semantic features  $\mathbf{p} \in \mathfrak{R}^{b \times h \cdot w}$ , which consists of a ResNet-152 model and a LSTM layer [20]. The segmentation feature module uses a pre-trained semantic image segmentation network, SPNet [21]

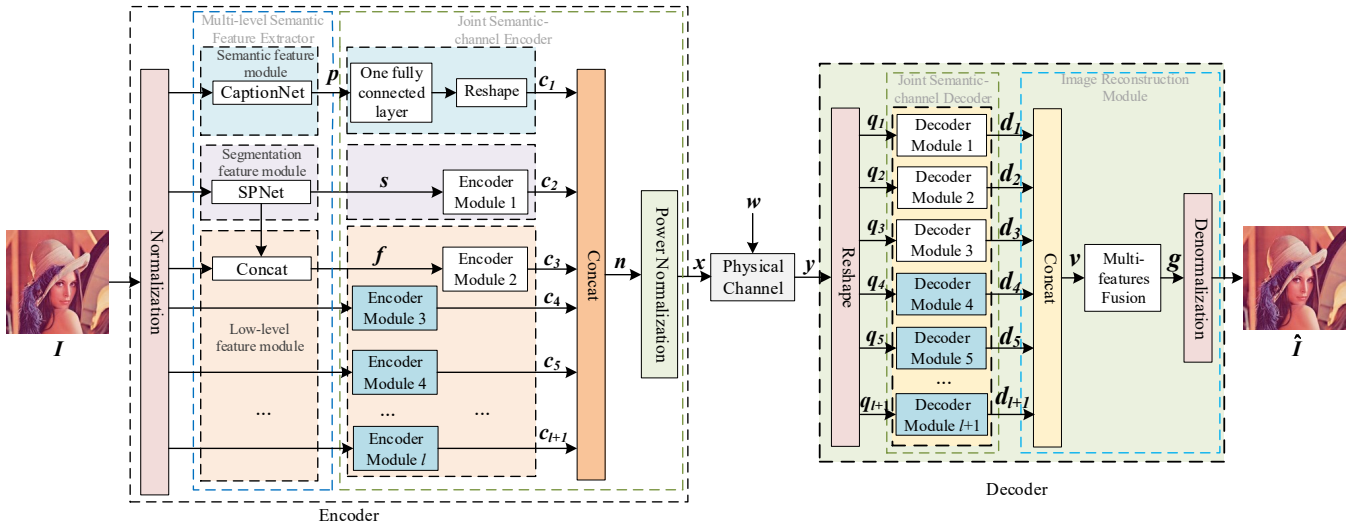


Fig. 2. The overall architecture of the proposed semantic communication system, MLSC-image.

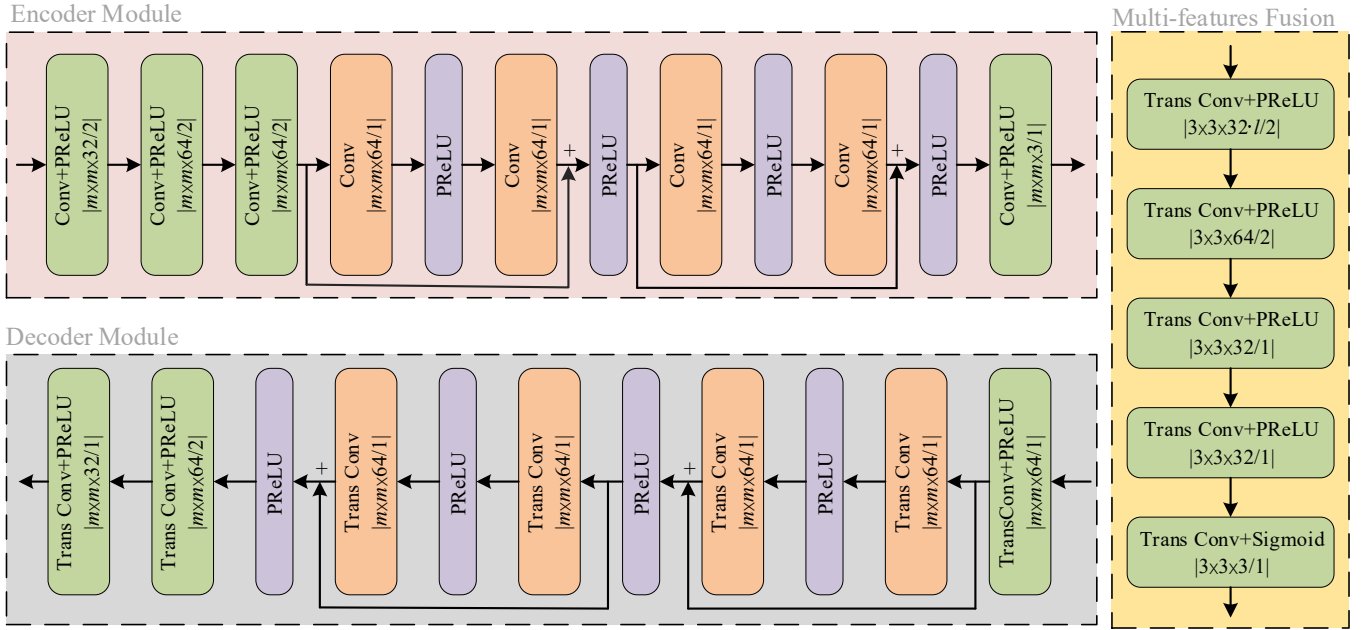


Fig. 3. The architecture of the Encoder Module, the Decoder Module and the Multi-features Fusion Module, the convolution neural networks are parameterized by  $m \times m \times c/s$ , where  $m$ ,  $c$  and  $s$  are kernel size, the number of channel outputs, and the stride, respectively. Each convolutional is followed by a batch normalization layer, which we omit here due to the space limitation.

to obtain the high-level segmentation features  $s \in \mathcal{R}^{b \times h \times w \times 3}$ . Then, the low-level feature module consists of  $l+1$  components: the Concat part, which concatenates the normalized image and the segmentation result, and outputs  $f \in \mathcal{R}^{b \times h \times w \times 6}$ , and  $l-2$  repeated direct input of the normalized image. This module aims to extract low-level semantic features, such as local details of the images. The hyperparameter  $l$  governs how many complementary details of the image to be transmitted to the receiver. This controls the trade-off between the quality of the reconstructed image and the transmission cost. The larger the  $l$  is, the better reconstruction will be, and vice versa.

These semantic features are then input to the semantic-channel encoder to be encoded into transmitted symbols.

### B. Joint Semantic-channel Encoder and Decoder

The joint semantic-channel encoder takes in four types of input: the text-form features  $p$ , the semantic image segmentation  $s$ , the concatenated features  $f$ , and the normalized image. The semantic features  $p$  is fed into a fully connected layer to reduce the dimension, followed by a reshape layer, which outputs  $c_1 \in \mathcal{R}^{b \times \frac{h}{t} \times \frac{w}{t} \times 1}$ , where  $t$  is the downsampling factor. The semantic features  $s$  and  $f$  fed into two encoder modules,

respectively. The structure of the module is presented in Fig. 3. These two encoder modules generate outputs of the same dimension, i.e.,  $\mathbf{c}_2 \in \mathfrak{R}^{b \times \frac{h}{t} \times \frac{w}{t} \times 3}$  and  $\mathbf{c}_3 \in \mathfrak{R}^{b \times \frac{h}{t} \times \frac{w}{t} \times 3}$ . The encoder module  $i$  ( $i=3, \dots, l$ ) shares the same model shown in Fig. 3 with various kernel sizes that  $m = 2 \times i - 3$ . Each of these modules takes the normalized image directly as the input, and output  $\mathbf{c}_{i+1} \in \mathfrak{R}^{b \times \frac{h}{t} \times \frac{w}{t} \times 3}$ ,  $i=3, 4, \dots, l$ . Then a concatenation layer combines the compressed features  $\mathbf{c}_1 \dots \mathbf{c}_{l+1}$  to  $\mathbf{n} \in \mathfrak{R}^{b \times \frac{h}{t} \times \frac{w}{t} \times (3 \times l + 1)}$ . Afterward, a power-normalization layer is applied to generate  $k$  complex transmitted symbols  $\mathbf{x}$  and regulate the transmitting power of these symbols to be under the given value where  $\mathbf{x} \in \mathbb{C}^{b \times k}$  and  $k = \frac{h}{t} \times \frac{w}{t} \times (3 \times l + 1)$ .

The reshape layer at the receiver first reshaped the received signals into size of  $b \times \frac{h}{t} \times \frac{w}{t} \times (3 \times l + 1)$  and then separates different-level semantic features  $\mathbf{q}_i$  from the received signals,  $i = 1, \dots, l + 1$ . More specifically,  $\mathbf{q}_1$  takes the first element of the last dimension of the reshaped symbols such that  $\mathbf{q}_1 \in \mathfrak{R}^{b \times \frac{h}{t} \times \frac{w}{t} \times 2}$ , where the last dimension is doubled as we concatenate the real and imaginary parts of the received symbols. Similarly,  $\mathbf{q}_i$  takes the  $3i - 1$ th to  $3i + 1$ th elements of the last dimension of the reshaped symbols such that  $\mathbf{q}_i \in \mathfrak{R}^{b \times \frac{h}{t} \times \frac{w}{t} \times 6}$ . Each of  $\mathbf{q}_i$ ,  $i = 1, \dots, l + 1$  is then input to a Decoder Module, the structure of which is shown in Fig. 3. The Decoder Module 1 2 and 3 have the same kernel size ( $m=3$ ), while the Decoder Module  $i$  has the kernel size of  $m = 2 \times i - 5$ ,  $i = 4, \dots, l + 1$ , corresponding to the encoder modules at the transmitter. Then each of the decoder modules output the reconstructed semantic features  $\mathbf{d}_i \in \mathfrak{R}^{b \times \frac{2h}{t} \times \frac{2w}{t} \times 3}$ ,  $i = 1, \dots, l + 1$ .

### C. Image Reconstruction Module

The output features  $\mathbf{d}_i$  from the decoder modules are first combined by a concatenation layer into  $\mathbf{v} \in \mathfrak{R}^{b \times \frac{2h}{t} \times \frac{2w}{t} \times 3 \cdot l + 1}$ . A Multi-features fusion module, as shown in Fig. 3, is used for the image reconstruction. Specifically, this module consists of several transpose convolutional layers with PReLU activation (sigmoid activation in the last layer), which outputs  $\hat{\mathbf{I}}$  that having the same size as the input image  $\mathbf{I}$ . Finally, a denormalization layer multiplies each value of  $\hat{\mathbf{I}}$  by 255 to generate the pixel value within the RGB range.

## IV. NUMERICAL RESULTS

We evaluate the proposed system using MSCOCO [22] and ADE20K [23] datasets. The MSCOCO dataset contains 123287 images (82783 for training and 40504 for validation, respectively). Each image is associated with five different captions. The ADE20K dataset contains 27574 images of 150 semantic labels with at least 512 pixels in height and width. Note that each image is cropped into a fixed size of  $h = 256$  and  $w = 256$  for training.

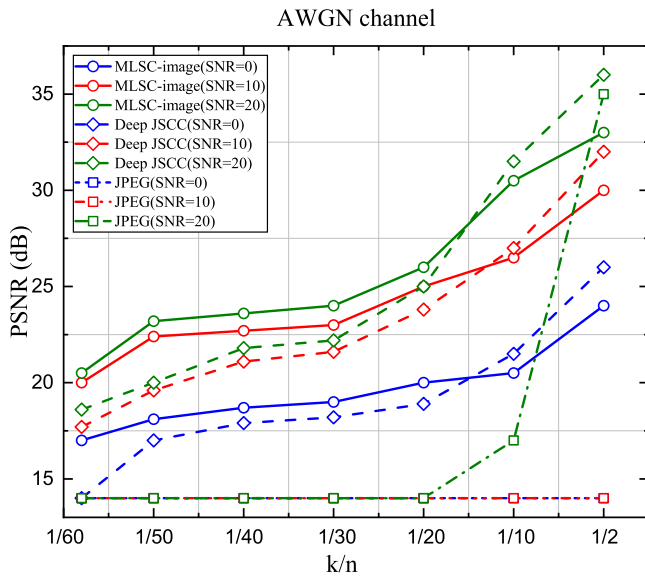
The proposed model was implemented in Pytorch and optimized using the Adam algorithm [24]. We set the learning rate to be 0.001, the batch size to be 32, and the down-sampling factor  $t=8$ , respectively. We adopt the existing DL-based method [12], referred to as Deep JSCC, and traditional

separation-based digital transmission schemes (JPEG) as the baseline to compare with, and use the PSNR and SSIM metrics to evaluate performance [25]. However the JPEG scheme has the minimum rate of compression, denoted by  $R_{min}$ , that is, if an image is compressed with a rate below  $R_{min}$ , then the JPEG scheme is not able to reconstruct the image but a random image instead. We have the maximum rate under given channel SNR  $R_{max} = \frac{k}{n} \log_2(1 + \text{SNR})$ , where  $k$  is the number of transmitted symbols, i.e., the number of channel use, and  $n$  is the number of pixels in the input image. In this experiment, if  $R_{min} > R_{max}$ , the JPEG scheme fails to work and generates random images, otherwise it compresses and reconstructs the images with the maximal rate it can works on below  $R_{max}$ . Note that we assume the transmission operates at channel capacity, which means that any explicit practical channel coding and modulation schemes have worse performance than this scheme for JPEG approach.

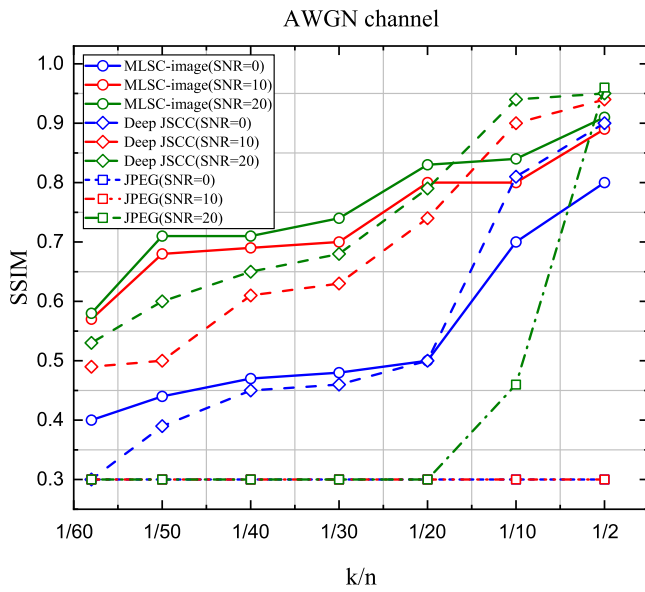
Fig. 4(a) shows the performance comparison with regards to different values of  $k/n$  with different SNR values in terms of PSNR, which shows that MLSC-image outperforms Deep JSCC and traditional image compression method JPEG. We also observe that DL-based image communication systems do not suffer from unexpected performance degradation from the ‘‘cliff effect’’. It can be seen that the digital transmission schemes would break down in poor channel conditions ( $\text{SNR} < 10\text{dB}$ ) and high compression ratio regime ( $k/n < 1/10$ ), while the DL-based systems still work. We note that the Deep JSCC scheme yields a higher PSNR score than the MLSC-image in the low compression ratio regimes since the transmitter has plenty of bandwidth to convey more detailed information of the image. However the proposed MLSC-image outperform the Deep JSCC scheme when  $k/n$  is small. This is due to that the proposed method is able to transmit more significant high-level semantic information with the limited bandwidth.

We present the performance comparison of different approaches in terms of SSIM in Fig. 4(b) under the same setting. The SSIM score reflects the similarity between original and reconstructed images from structural aspects. We observe a similar trend that the proposed MLSC-image remarkably outperforms the other counterparts in low  $k/n$  regime, while performs worse than Deep JSCC in the high  $k/n$  regime, which further demonstrate the advantages of the proposed scheme under the limited bandwidth condition.

We then evaluate the robustness of the MLSC-image scheme under different channel conditions. Specifically, we train the proposed model under channels with a specific SNR value, while testing with various SNR values, the results of which is presented in Fig. 5. Note that during the  $\text{SNR}_{\text{test}} < \text{SNR}_{\text{train}}$  situation, the MLSC-image system does not suffer from the ‘‘cliff effect’’, which often is observed by the digital transmission scheme. Instead, the MLSC-image system exhibits a steady degradation of performance with the decrease of the SNR value. We can also observe that the reconstructed image quality of the proposed MLSC-image has increased until the performance finally saturates with the  $\text{SNR}_{\text{test}}$  increases. It



(a)



(b)

Fig. 4. Performance comparison of different approaches over an AWGN channel with different compression ratios ( $k/n$ ) and SNR values in terms of (a) PSNR and (b) SSIM.

exhibits an apparent tradeoff between the compression and the robustness of the proposed method, where if the model is trained with high SNR, the PSNR performance of the system is mainly determined by the bandwidth compression ratio, while otherwise, the system is robust to different channel conditions.

Fig. 6 compares the PSNR performance of the alternative MLSC-image architectures without the semantic feature module or segmentation feature module. The results show that both of the two modules improve the performance of the proposed system, which is more significant in the low SNR regime. This further validates the benefits of high-level text and

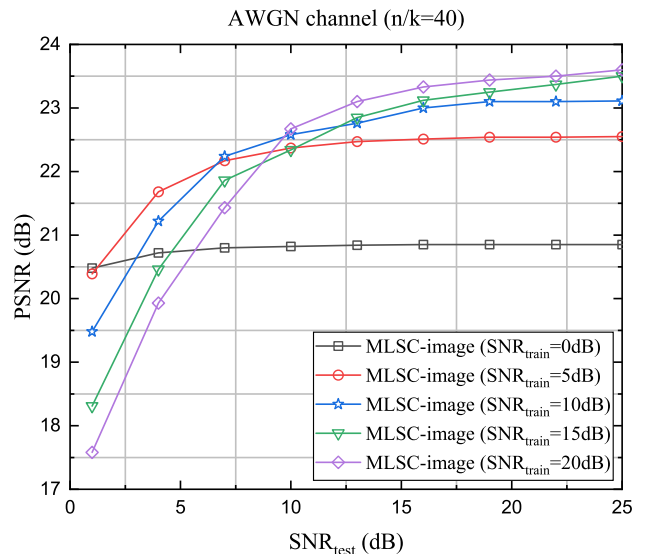


Fig. 5. PSNR performance of the MLSC-image algorithm over an AWGN channel with training on a specific channel SNR value and testing on the varying SNR values.

segmentation semantic in the compression and transmission of images. We also note that the degradation of the performance by the model without the segmentation feature module is more obvious than that by the model without the semantic feature module, which indicates that segmentation related feature is of higher semantic importance.

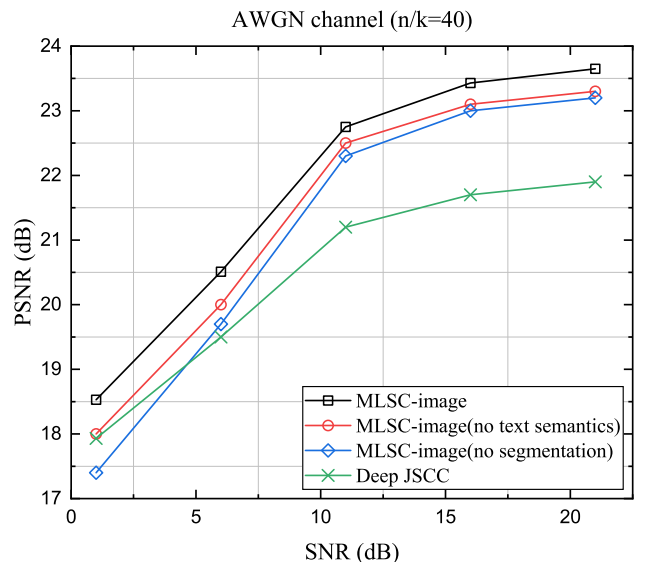


Fig. 6. Performance of alternative MLSC-image architectures over an AWGN channel with riding caption or image segmentation.

## V. CONCLUSION

In this paper, we proposed a novel DL-enabled semantic communication system for wireless image transmission, named MLSC-image. We jointly design the transmitter and

receiver to reconstruct the source information, which achieves a remarkable performance than Deep JSCC and traditional separation-based digital transmission schemes. Additionally, the multi-level semantic feature extractor is used for extracting abundant features of the image with different forms. Simulation results demonstrated that the MLSC-image performance is worse than Deep JSCC due to the abundant bandwidth transmitting more detailed information in the low compression ratio situation. However, the MLSC-image shows the importance of the construction features in the high compression ratio situation, especially in the low SNR regime.

## REFERENCES

- [1] C. E. Shannon, "A mathematical theory of communication," *Bell Syst. Tech. J.*, vol. 27, pp. 379–423, Jul. 1948.
- [2] E. C. Strinati, S. Barbarossa, "6G networks: Beyond Shannon towards semantic and goal-oriented communications," *Comput. Networks*, vol. 190, 2021.
- [3] E. C. Strinati, D. Belot, A. Falempin and J. -B. Doré, "Toward 6G: From New Hardware Design to Wireless Semantic and Goal-Oriented Communication Paradigms," *IEEE European Solid State Circuits Conf., Proc.*, pp. 275-282, 2021.
- [4] C.-X. Wang, J. Huang, H. Wang, X. Q. Gao, X.-H. You, and Y. Hao, "6G oriented wireless communication channel characteristics analysis and modeling," *Chinese J. Int. Things*, vol. 4, no. 1, pp. 19–32, Mar. 2020.
- [5] G. Shi, Y. Xiao, Y. Li and X. Xie, "From Semantic Communication to Semantic-Aware Networking: Model, Architecture, and Open Problems," *IEEE Commun. Mag.*, vol. 59, no. 8, pp. 44-50, Aug. 2021.
- [6] P. Basu, J. Bao, M. Dean, and J. Hendler, "Preserving quality of information by using semantic relationships," *Pervasive Mob. Comput.*, vol. 11, pp. 188–202, Apr. 2014.
- [7] H. Xie and Z. Qin, "A Lite Distributed Semantic Communication System for Internet of Things," *IEEE J. Sel. Areas Commun.*, vol. 39, no. 1, pp. 142-153, Jan. 2021.
- [8] H. Xie, Z. Qin, G. Y. Li and B. -H. Juang, "Deep Learning Enabled Semantic Communication Systems," *IEEE Trans. Signal Process.*, vol. 69, pp. 2663-2675, 2021.
- [9] N. Farsad, M. Rao, and A. Goldsmith, "Deep learning for joint source-channel coding of text," *Proc. IEEE Int. Conf. Acoust., Speech Signal Process. (ICASSP)*, Calgary, AB, Canada, pp. 2326–2330, Apr. 2018.
- [10] Z. Weng and Z. Qin, "Semantic Communication Systems for Speech Transmission," *IEEE J. Sel. Areas Commun.*, vol. 39, no. 8, pp. 2434–2444, Aug. 2021.
- [11] H. Tong, Z. Yang, S. Wang, Y. Hu, O. Semiari, W. Saad, and C. Yin, "Federated Learning for Audio Semantic Communication," *Frontiers in Communications and Networks*, vol. 2, Sep. 2021.
- [12] E. Bourtsoulatzé, D. Burth Kurka and D. Gündüz, "Deep Joint Source-Channel Coding for Wireless Image Transmission," *IEEE Trans. Cognit. Commun. Networking*, vol. 5, no. 3, pp. 567-579, Sep. 2019.
- [13] H. Qiu, Q. Zheng, G. Memmi, J. Lu, M. Qiu and B. Thuraisingham, "Deep Residual Learning-Based Enhanced JPEG Compression in the Internet of Things," *IEEE Trans. Ind. Inf.*, vol. 17, no. 3, pp. 2124-2133, Mar. 2021.
- [14] D. B. Kurka and D. Gündüz, "Deepjssc-f: Deep joint source-channel coding of images with feedback," *IEEE J. Sel. Areas Inf. Theory*, vol. 1, no. 1, pp. 178–193, Apr. 2020.
- [15] M. Yang, C. Bian and H. -S. Kim, "Deep Joint Source Channel Coding for Wireless Image Transmission with OFDM," *IEEE Int Conf. Commun.*, Montreal, QC, Canada, pp. 1-6, 2021.
- [16] C.-H. Lee, J.-W. Lin, P.-H. Chen, and Y.-C. Chang, "Deep learning-constructed joint transmission-recognition for Internet of Things," *IEEE Access*, vol. 7, pp. 76547–76561, Jun. 2019.
- [17] M. Jankowski, D. Gündüz, and K. Mikolajczyk, "Wireless image retrieval at the edge," *IEEE J. Sel. Areas Commun.*, vol. 39, no. 1, pp. 89–100, Jan. 2021.
- [18] M. Jankowski, D. Gündüz, and K. Mikolajczyk, "Joint device-edge inference over wireless links with pruning," *Proc. IEEE 21st Int. Workshop Signal Process. Adv. Wireless Commun.*, Atlanta, GA, USA, pp. 1–5, May 2020.
- [19] X. Liu and Q. Xu, "Adaptive Attention-based High-level Semantic Introduction for Image Caption," *ACM Trans. Multimedia Comput. Commun. Appl.*, vol. 16, no. 4, Article 128, 22 pages, Jan. 2021.
- [20] K. He, X. Zhang, S. Ren and J. Sun, "Deep Residual Learning for Image Recognition," *Proc IEEE Comput Soc Conf Comput Vision Pattern Recognit (CVPR)*, pp. 770-778, 2016.
- [21] Q. Hou, L. Zhang, M. -M. Cheng and J. Feng, "Strip Pooling: Rethinking Spatial Pooling for Scene Parsing," *Proc IEEE Comput Soc Conf Comput Vision Pattern Recognit (CVPR)*, pp. 4002-4011, 2020.
- [22] T. Y. Lin, M. Maire, S. Belongie, J. Hays, P. Perona et al., "Microsoft coco: Common objects in context," *Proc. European Conf. on Computer Vision*, Zurich, Switzerland, pp. 740–755, 2014.
- [23] B. Zhou, H. Zhao, X. Puig, S. Fidler, A. Barriuso and A. Torralba, "Scene Parsing through ADE20K Dataset," *Proc. IEEE Conf. Comput. Vis. Pattern Recognit, (CVPR)*, pp. 5122-5130, 2017.
- [24] A. Paszke, S. Gross, F. Massa, A. Lerer, J. Bradbury, G. Chanan, T. Killeen, Z. Lin, N. Gimelshein, L. Antiga, et al. Pytorch: An imperative style, high-performance deep learning library. *Adv. neural inf. proces. syst.*, pp. 8024–8035, 2019.
- [25] Z. Wang, A. C. Bovik, H. R. Sheikh, and E. P. Simoncelli, "Image quality assessment: From error visibility to structural similarity," *IEEE Trans. Image Process.*, vol. 13, no. 4, pp. 600–612, Apr. 2004.